HAL
open science

Long-term trends of the concentration of the minor constituents in the mesosphere ? a model study

M. Grygalashvyly, G. R. Sonnemann, P. Hartogh

To cite this version:

M. Grygalashvyly, G. R. Sonnemann, P. Hartogh. Long-term trends of the concentration of the minor constituents in the mesosphere ? a model study. Atmospheric Chemistry and Physics Discussions, 2007, 7 (6), pp.15453-15494. hal-00303157

HAL Id: hal-00303157

https://hal.science/hal-00303157v1

Submitted on 18 Jun 2008

HAL is a multi-disciplinary open access archive for the deposit and dissemination of scientific research documents, whether they are published or not. The documents may come from teaching and research institutions in France or abroad, or from public or private research centers.

L'archive ouverte pluridisciplinaire **HAL**, est destinée au dépôt et à la diffusion de documents scientifiques de niveau recherche, publiés ou non, émanant des établissements d'enseignement et de recherche français ou étrangers, des laboratoires publics ou privés.

Atmos. Chem. Phys. Discuss., 7, 15453–15494, 2007
www.atmos-chem-phys-discuss.net/7/15453/2007/
© Author(s) 2007. This work is licensed
under a Creative Commons License.

Atmospheric Chemistry and Physics Discussions

Long-term trends of the concentration of the minor constituents in the mesosphere – a model study

M. Grygalashvyly[1], G. R. Sonnemann[1,2], and P. Hartogh[2]

[1]Leibniz-Institute of Atmospheric Physics at the University Rostock in Kühlungsborn, Schloss-Str. 6, 18225 Ostseebad Kühlungsborn, Germany
[2]Max-Planck-Institute for Solar System Research, Max-Planck-Str. 2, 37191 Katlenburg-Lindau, Germany

Received: 12 October 2007 – Accepted: 22 October 2007 – Published: 2 November 2007

Correspondence to: M. Grygalashvyly (gryga@iap-kborn.de)

Abstract

We investigate the influence of the rising concentrations of methane, dinitrogen oxide and carbon dioxide since the pre-industrial era upon the chemistry of the mesosphere. We use for calculations our global 3D-model COMMA-IAP designed for the exploration of the MLT-region and particularly the extended mesopause region. In order to get approximated data of the solar Lyman-α flux back to the pre-industrial time, we derived a quadratic fit using the sunspot number available since 1749 as the only solar proxy for the Lyman-α flux before 1947. The Lyman-α flux values are employed to determine the water vapor dissociation rate. The water vapor trend analysis utilizes estimated methane trends since the pre-industrial era. An unsolved problem for the model calculations consists of the water vapor mixing ratio at the hygropause during the time range of trend calculation. We assume that the hygropause was dryer at the pre-industrial time than currently. As a consequence of the methane oxidation, the middle atmosphere became more humid according to the rising methane concentration, but depending on height and with a small time delay of few years. The solar influence on the water vapor mixing ratio is insignificant below about 80 km within summery high latitudes, but it becomes increasingly more important above this altitude. The growing water vapor concentration increases the hydrogen radical concentration and reduces the mesospheric ozone. A second region of stronger ozone decrease is located in the vicinity of the stratopause. Increasing CO_2 concentration enhances slightly the concentration of CO in the mesosphere, but its influence upon the chemistry is small and its main effect is connected with a cooling of the upper atmosphere. We discuss the trends particularly in view of the impact on the NLC region.

1 Introduction

Trend is the tendency of the change of a parameter within a sufficiently long time period eliminating all accidental (natural) and quasi cyclic variations. In view of the atmo-

ACPD

7, 15453–15494, 2007

sphere, dominant cyclic variations are the annual variation or the quasi 11-year solar activity cycle (Schwabe-cycle). The quasi biennial oscillation (QBO), the North Atlantic oscillation (NAO), and the El Nio southern oscillation (ENSO) phenomenon also belong to quasi cyclic oscillations. In order to infer a long-term trend, the elimination of the influence of these variations is not a simple task. A serious problem also exists in the search for the reason for a detected trend and, in case more than one impact influences the trend, the assessment of the magnitude of the individual impacts. In particular, we observed and derived an increase of the concentration of different minor constituents in the atmosphere since the beginning of industrialization. However the solar activity outside of the Schwabe-cycle (e.g., the Geisberg-cycle of an approximate century time-scale) and maybe other natural variations have changed since then. We now detect that other parameters, such as the temperature or the water vapor concentration, have certain trends. Thus, we have to assess the shares from the different impacts. In the frame of sophisticated models one can try to find an answer, being aware that no model will give a final answer to all open questions.

We use for calculation our global three-dimensional model of the middle atmosphere COMMA-IAP (COlogne Model of the Middle Atmosphere of the Institute of Atmospheric Physics in Kühlungsborn, 0–150 km). The model was particularly designed to investigate the spatio-temporal structure of phenomena in the MLT-region (mesosphere/lower thermosphere) and especially in the extended mesopause region. The coupled dynamic-chemical transport model was described in more detail in, among other publications, Berger (1994), Ebel et al. (1995), Sonnemann et al. (1998), Kremp et al. (1999), Berger and von Zahn (1999), Körner and Sonnemann (2001), and Hartogh et al. (2004). Our main goal is the reproduction of the water vapor trend in the middle atmosphere on the basis of the derived and measured trends of methane (CH_4), dinitrogen oxide (N_2O), and carbon dioxide (CO_2) inclusive of the trend of the solar Lyman-α radiation. We also consider the effect on mesospheric ozone and other minor constituents and the chemical heating rate. We exclude the investigation of the impact on the stratospheric chemistry with exception of the stratopause region. Special atten-

tion is paid to the season and domain of the occurrence of noctilucent clouds (NLC) and polar mesospheric summer echoes (PMSE). Here we exclude the consideration of the NO_x-problem although the formation of NO_x due to the oxidation of N_2O by $O(^1D)$ is included in the model.

2 Derived trend data

Direct measurements of atmospheric minor constituents are available for the recent past only. The same is valid for the solar output. There are different indirect data and estimations. The so-called pre-industrial level of methane has been estimated to be by 0.75–0.85 ppmv (roughly half the present value) (World Meteorological Organization, 1999). The present value ranges by 1.75 ppmv (Dlugokencky et al., 2003). The increase was essentially exponential but for the latest two decades or so a decline of the growing rate has been observed (Khalil et al., 1993; Dlugokencky et al., 2003) which seems to be zero for the latest years. Despite the slow down of the methane growing rate, we use for calculation a constant rate between 1880 and the now, enhancing methane from 0.825 to 1.7 ppmv. As methane is not subjected to the freeze-dry process at the tropopause, in contrast to water vapor, the increasing methane concentrations due to intensification of rise cultivation in marshland, stock-breeding, and further anthropogenic sources can penetrate into the middle atmosphere.

The N_2O concentration is likewise rising since the time of the intensification of agriculture. We also take into consideration an exponential increase of its concentration from a pre-industrial level at the surface of 254 ppmv to the current value of 324.2 ppmv. However, we do not consider in detail the problem of rising NO_x concentrations due to N_2O oxidation because it requires more care in modeling (careful estimation of thermospheric sources and of the formation by cosmic rays, modeling of the stratosphere/troposphere exchange processes on the basis of a full code of the stratosphere chemistry). The increase of the CO_2 concentration is best investigated. There is generally an exponential growth of its concentration but with some variations in its growth

rate. The growth rate mirrors the world wars or the oil crises, etc. The pre-industrial level at the ground is estimated to be 280 ppmv. The recent value amounts to about 375–380 ppmv (in 2006).

3 Trend of the Lyman-α radiation

The Lyman-α insolation is the most important radiation dissociating water vapor above the middle mesosphere (roughly above 70 km) varying strongly with solar activity. The absolute amount and the relative variation of the Lyman-α radiation have recently been corrected (Woods et al., 2000). The old values used by the scientific community were based on measurements by Vidal-Madjar (1975, 1977), Vidal-Madjar and Phissamay (1980), and Simon (1981). The standard flux value for mean solar activity was 3×10^{11} photons $cm^{-2}s^{-1}$ and the variation from solar minimum to maximum amounted to a factor of 2. The latest values, based on UARS measurements according to Woods et al. (2000), amount to 4.65×10^{11} photons $cm^{-2}s^{-1}$ for a mean value and the radiation varies between 3.7 and 5.6×10^{11} photons $cm^{-2}s^{-1}$ averaged over two years. In the domain below about 75 km, the radiation within the Schumann-Runge band system becomes increasingly important. Depending on the wavelength, the radiation varies by only a few percentage points. The longer the wavelength is, the smaller the variation. There was an increase in solar activity since the time of the first observation of NLC in 1883 as the sunspot number or the geomagnetic activity verifies. However, direct Lyman-α measurements are only available for the last three solar cycles.

In order to reproduce the solar output of the Lyman-α radiation, different solar proxies have been employed. Woods et al. (2000) used direct measurements by means of different satellites such as the AE-E, SME and UARS and filled the data gaps by employing solar proxies. The radiation has been reconstructed back to 1947 using the solar 10.7 cm flux as proxy available since that year. The only available direct or indirect solar proxies before 1947 are the sunspot numbers (since 1749) and the geomagnetic activity (aa-index since 1868). It is true the geomagnetic activity varies with

the solar activity indicated by the sunspot number, but there is a time delay of about two years between sunspot number and geomagnetic activity. Surprisingly, this phase shift seems to agree with a delay of the occurrence rate of NLC (Gadsden, 1998; Thomas and Olivero, 2001). However, this assertion seems to be still under discussion. Also, Thomas and Olivero (2001) used the sunspot number as proxy and calculated the Lyman-α flux on the basis of a quadratic fit. We also used the sunspot number as a proxy for the Lyman-α flux and quadratically fitted the sunspot number values to the Lyman-α flux values given by Woods et al. (2000). From this procedure we obtained a quadratic formula which can then be employed for the time range before 1947. Comparing the measured Lyman-α flux with the sunspot number, the correlation between both is poor for time scales in the order of few rotation periods of the sun or shorter, but this is not true for time scales in the order of a year. That is why we smooth the sunspot number over 11 months. For the Lyman-α flux we derived the expression

$$\Phi(L\alpha) = (3.396 + 1.71419 \times 10^{-2} S - 1.68423 \times 10^{-5} S^2) \times 10^{11} \text{photons cm}^{-2}\text{s}^{-1} \quad (1)$$

S stands for the 11-month smoothed sunspot number. Figure 1 shows the result of adjustment. The values vary coarsely between 3.5 and 5.8×10^{11} photons $\text{cm}^{-2}\text{s}^{-1}$ with exception of the strongest cycle which is at maximum in 1957. One recognizes a general trend of increase in the maximum (and mean) values until the middle of the past century, but after that a decrease begins. It is important to note that the minima display only a weak increasing trend. Thus we use these values for comparison of the change in composition of the minor constituents.

4 Water vapor mixing ratio at the hygropause

The hygropause separates the wet troposphere from the dry middle atmosphere. The water vapor concentration is subjected to a freeze-dry process and its concentrations drop from some hundred ppmv in the troposphere to approximately 4 ppmv above the hygropause. We use the water vapor mixing ratio above the hygropause as a lower

boundary condition because we cannot simulate the complicated tropospheric water vapor content and the freeze-dry process in the frame of our model. In order to calculate the water vapor trend of the middle atmosphere we have to consider the possible trend of the lower boundary conditions. Evidence for a changing hygropause was given by Foster and Shine (1999). A strong increase of the stratospheric water vapor was found in the most recent past (Oldmans and Hofmann, 1995; Evans et al., 1998) which could only be explained to 40% by the methane increase (Foster and Shine, 1999). We can take this as an indication that the pre-industrial hygropause was essentially dryer than now and will discuss it in the following section. The reason may result from two facts. Firstly, the globally averaged water vapor flux within the stratosphere is directed downward (Sonnemann and Körner, 2003). It is a common erroneous belief that water vapor enters, on global average, into the stratosphere from the troposphere. The truth is that methane moves advectively and diffusively through the tropopause into the middle atmosphere and will there be oxidized to water vapor, forming a water vapor mixing ratio maximum close to the stratopause. An upward and downward directed water vapor flux results from this peak. This is the global mean picture which, of course, can differ locally or temporally. The increase with height of the globally averaged water vapor mixing ratio is characterized by a certain positive gradient. The question arising from this fact is does the gradient essentially depend on the magnitude of the water vapor maximum at the stratopause or is it in first approximation a conservative quantity? In the second case, the hygropause becomes proportional to the water vapor increase more humid and in the first extreme case, if the water vapor mixing ratio (mr) at the hygropause is a conservative quantity (actually an unrealistic picture), the gradient of the water vapor mixing ratio ($d[H_2O]_{mr}/dz$) becomes larger.

Secondly, due to the increase of the concentrations of the different greenhouse gases, the troposphere becomes warmer and, as a consequence of this, becomes more humid. Water vapor is the most important greenhouse gas but it is triggered by the other greenhouse gases (CO_2, CH_4, N_2O, O_3, etc.) of which concentrations rise owing to anthropogenic activity. Thus, the humidity at the hygropause should increase

based on the change of the tropospheric conditions. However, these simple arguments provide only a qualitative answer and this goes: the hygropause was dryer in the pre-industrial time than currently but we cannot determine the true value thus far. We tend to take into calculation a conservative value of a 10% dryer hygropause than presently exists.

5 Chemical aspects

As mentioned above, methane is finally oxidized to water vapor or decomposed to molecular hydrogen. Although a branch of the methane decomposition results in H_2, its concentration does not essentially change with height in the stratosphere as it is oxidized by OH or $O(^1D)$ to H_2O. The methane decomposition starts with a reaction with OH or $O(^1D)$. The intermediate compounds of the methane decomposition will not be considered in the global model, but, according to Sonnemann et al. (1998), we use the initial decomposition reaction as a measure for the final products. The partitioning depends on the concentrations of atomic oxygen, NO and O_2 as well as the dissociation rates of H_2CO resulting in $CO+H_2$ or HCO+H. In other words, the initial reaction determines the life time of methane, and the follow-up reactions take place very fast. Although molecular hydrogen results from the methane decomposition its mixing ratio is almost constant in the stratosphere. The reason consists in an autocatalytic H_2 oxidation to water vapor (Sonnemann et al., 2005a). Since the oxidation of H_2O by $O(^1D)$ is the main source of the

OH-radicals in the stratosphere, the methane destruction forming H_2O becomes faster the more humid the atmosphere is, meaning the more methane is available. $O(^1D)$ results from the dissociation of ozone. At least, within the mesosphere, the hydrogen radicals decompose ozone so that a negative feedback occurs there. The ozone destruction entails a smaller $O(^1D)$ production and that reduces the hydrogen radical formation. However, in the mesosphere the photolysis of water vapor, being the hydrogen radical source, becomes more important with increasing altitude compared

with the influence of $O(^1D)$. Therefore, we expect a decrease of the ozone concentration if the water vapor concentration increases, particularly in the upper mesosphere and the mesopause region but also in the stratopause region, whereas the region between these domains is not so strongly affected. The reason is given, essentially, by two odd oxygen destructing cycles. In the upper mesosphere and mesopause region, ozone destroying cycle involving atomic hydrogen acts:

$$O_3 + H \rightarrow O_2 + OH \quad (2)$$

$$OH + O \rightarrow H + O_2 \quad (3)$$

$$\text{net}: O + O_3 \rightarrow 2O_2 \quad (4)$$

This is a very effective cycle declined in the middle mesosphere by the fact that H will be removed from the atmosphere because it is subjected to the three-body reaction $H+O_2+M \rightarrow HO_2+M$ depending quadratically on the air density. In the middle mesosphere increasing toward the stratopause region, a second cycle becomes increasingly important:

$$H + O_2 + M \rightarrow HO_2 + M \quad (5)$$

$$HO_2 + O \rightarrow OH + O_2 \quad (6)$$

$$OH + O \rightarrow H + O_2 \quad (7)$$

$$\text{net}: O + O \rightarrow O_2 \quad (8)$$

O results from the dissociation of ozone so that this cycle ozone reduces. The relative effect is largest at or a little above the stratopause. Due to the small reaction rate the Chapman reaction $O+O_3 \rightarrow 2O_2$ plays no a great role in the mesosphere. The process becomes more important below the stratopause where the ozone concentration still strongly increases. The reaction is not directly influenced by an increasing humidity,

but indirectly, if the concentrations of O and the composition between both constituents, O and O_3, change by the influence of the hydrogen radicals. Within the stratosphere the impact of enhanced water vapor concentration is not simple to estimate, since the reactions of OH with the chlorine and nitrogen radicals, decomposing ozone and resulting in neutral HCl and HNO_3, have to be taken into consideration. Here we do not consider the response of increasing H_2O mixing ratios on the stratospheric ozone chemistry.

The rising N_2O concentration influences the NO concentration in the middle atmosphere. The oxidation of N_2O by $O(^1D)$, particularly in the stratosphere, results in the formation of two NO molecules. The global middle atmospheric circulation also conveys NO from the stratosphere into the D-layer in moderate and high latitudes in summer whereas the transport in low and equatorial latitudes is more complicated. In a large number of contributions (e.g., Taubenheim, 1997; Bremer, 1997, 2001; Bremer and Berger, 2002) the descent of the so-called reflection height of radio-waves has been used as a tracer for middle atmospheric cooling. In contrast to the lower atmosphere, CO_2 cools the upper atmosphere, entailing a decrease of the levels of constant air density. The reflection height is determined approximately by a constant level of electron density. It is assumed, if the solar activity is taken into consideration in the calculations, that in a first approximation a constant level of electron density is connected with a constant level of air density. The electron density within the D-layer is a function of the NO density, and within the water clusters region (below about 85 km), the formation of water clusters depends additionally on the water vapor and CO_2 concentrations. Thus, the estimation of the direct influence of the trends of all minor constituents upon the D-layer should be of great interest. As mentioned, a careful investigation of all influences impacting the D-layer is required to give a definitive answer.

The increase of the CO_2 concentration is jointly responsible for the warming of the troposphere and the cooling of the atmosphere above. The direct influence upon the chemistry is very small below the upper mesosphere. CO_2 is increasingly dissociated

into CO and O in the mesosphere. CO reacts with OH and returns to CO_2. Only a radical conversion takes place in this reaction from OH to H which influences the ozone chemistry rather marginally. As mentioned above, the most important impact is connected with the ion-chemistry. The model under consideration does not operate interactively. Hence, we do not consider the CO_2 increase in the dynamic model but only in the chemical transport model. In other words, the change of the dynamical parameters such as temperature and global circulation is not taken into account.

6 Results

6.1 Impacts due to the methane increase

From a chemical point of view, the rising methane concentration is the most important anthropogenic increase of a minor constituent in the mesosphere. The total hydrogen content, meaning the number of hydrogen atoms anywhere bound in molecules, is a conservative quantity up to the height where molecular diffusion begins effectively to act. Methane is an effective carrier of hydrogen. It is completely decomposed in the atmosphere. There is no formation process for methane in the atmosphere. Figure 2a displays a seasonal section of the diurnally averaged water vapor mixing ratio at 67.5° N in 1890 – the solar minimum year at the beginning of the increase of the methane mixing ratio – calculated by means of COMMA-IAP. This is also approximately the time of the eruption of the volcano Krakatoa (1883). Before this date no NLC have been observed. Figure 2b exhibits the same state of affairs for 1997, nearly the end of the considered time interval. We compare, as mentioned, only years of minimum solar activity (1890 and 1997) with each other because for non-minimum years the radiation conditions are too different. Figure 3 shows the annual variation of a 7-day sliding mean of the water vapor mixing ratio at ALOMAR (69.29° N), Norway, measured by the microwave facility (Hartogh and Hartmann, 1990; Hartogh et al., 1991; Hartogh and Jarchow, 1995; Hartogh, 1997; Seele and Hartogh, 1999; Hartogh et al., 2004)

in 1998 close to the year of minimum (the measurements at ALOMAR in 1997 were interrupted for a longer space of time). Comparing both figures – the calculations and observations – one will find that they agree in the typical annual patterns and that the mixing ratios are also quantitatively reproduced.

Figure 4 depicts the calculated annual variation of the relative deviation (rd) of a diurnally averaged water vapor mixing ratio between 1997 and 1890 at 67.5° N according to the expression rd=$(mr_{1997}-mr_{1890})/mr_{1890}\times 100$ [%]. Up to 85 km, the water vapor trend is generally positive. There is a range of slightly decreasing water vapor mixing ratios above this border in September/October, whereas the increase is very strong in this domain from January until April. The absolute values are very small there so that weak changes entail large relative variations. The main reason for this behavior is the fact that the Lyman-α radiation also slightly increased during the years of solar activity minimum and thus it was higher in 1997 than in 1890. The relative deviations in a latitudinal section for north summer solstice and north spring equinox are shown in Figs. 5a and b respectively. The figures demonstrate that the relative increase of the middle atmospheric humidity depends on altitude, latitude and season. The strongest deviations occur just in the mesopause region. In the region of NLCs and PMSEs in high summery latitudes marked by upward directed vertical winds, the relative deviations reach 35–45%. A reason for the strong relative deviation in the mesopause region may be given by the autocatalytic water vapor production below 65 km (Sonnemann et al., 2005a) and the meridional transport. The more humid the atmosphere, the more effective the process of autocatalytic water vapor production.

The diurnal variation of the water vapor mixing ratio is not significant below 80 km, but above 80 km, in the region of NLC and PMSE formation, it becomes increasingly stronger. Figure 6a displays the altitude-time section of the water vapor mixing ratio at 67.5° N near north summer solstice (1 July) for midnight. One can recognize the general increase of the mixing ratio at constant height. Above about 80 km the solar cycle is clearly mirrored. Figures 6b and 6c show the same relations at middle and low latitude. One finds that the influence of the solar cycle penetrates essentially deeper at

lower latitudes. The reason is given by the global vertical wind patterns. The upward directed vertical wind in high and moderate latitudes during the summer season lifts air that is not strongly influenced by the variations in solar activity from the lower domain into heights where the variable Lyman-α radiation still penetrates. The comparison between the characteristic transport time and the characteristic time of photolysis is the decisive criterion for the amplitude of the variation with the solar cycle (Sonnemann and Grygalashvyly, 2004). In contrast, a downward wind, as appears during the winter season, conveys air strongly influenced by the variable Lyman-α radiation to lower heights.

Within the NLC region the impact of the solar radiation is reduced, but the amplitude of water vapor due to the solar cycle impact possesses a considerable gradient between 80 and 90 km. At 80 km only a small variation exists whereas a pronounced variation occurs at 90 km. Although the condensation germs for the NLC particles will be created in altitudes close to the temperature minimum at about 86 to 89 km, the NLC particles sediment and grow according to the surrounding water vapor mixing ratio, meaning the influence of the solar activity cycle on the NLC occurrence rate is dampened by the upward directed vertical wind. However, the temperature has the strongest influence on the growth of NLCs, but its variation with the solar cycle is not modeled.

Figures 7a and b display the increase of the water vapor mixing ratio at different selected mesospheric altitudes in high and low latitudes for summer solstice. The figures clearly show the different responses to the solar variation, particularly at 80 km. Increasing water vapor concentrations are a source for greater hydrogen radical concentrations and these entail a stronger loss of the odd oxygen constituents: atomic oxygen and ozone. Figures 8a and b depict the relative deviation of the diurnally averaged ozone concentration in a latitudinal section for north summer solstice and equinox conditions. Generally, the ozone concentration decreases the most, with the exception of an area in high latitudes around the mesopause. At and above the stratopause a further region of stronger ozone loss is recognized whereas the middle mesosphere is

less strongly impacted. A similar picture exhibits atomic oxygen (not shown).

The chemical system responds in a nonlinear manner in the mesopause region. This finding was investigated in a large number of publications by Sonnemann and coworkers and other groups. We refer only to Sonnemann and Grygalashvyly (2005) and quotations therein. As the latitudinal sections in Figs. 8a and b demonstrate, different regions of an ozone increase occur below the mesopause. The cause is a nonlinear response of the photochemical system. As the integration time step has to be relatively large for trend calculations (15 min) and, additionally, the odd oxygen species are treated as family, effects such as subharmonics or chaos cannot occur in the calculations as large time steps and the family concept suppress these phenomena (Sonnemann and Grygalashvyly, 2005 and quotations therein). Apparently the system tends to create a bistable behavior.

Figure 9 shows an example of the diurnally averaged ozone mixing ratios at 81 km altitude in two different latitudes for 1 January. A bistable behavior seems to occur which, in one case, appears under conditions of small water vapor concentrations and disappears for higher values, while, in the other case, it becomes dominant for larger water vapor concentrations. The behavior is triggered by the solar cycle. Figure 10 exhibits an example at 83 km altitude and 22.5° N latitude for 1 July. A clear decreasing ozone trend is recognizable, but beginning after 1930 a bistable response occurs. The possibility of a trigger solution under the condition of a hydrogen flux was discussed in Yang and Brasseur (1994). Our results may hint of a bistable behavior but, on the other hand, the integration of the system is too coarse to get a definitive answer.

Ozone decreases because the concentrations of the hydrogen radicals increase. As an example, Fig. 11 depicts the relative deviation of diurnally averaged hydroxyl mixing ratio according to the conditions shown in Fig. 8b (1 April). The OH-layer is located in the mesopause region. Figure 12 displays its increasing trend of diurnally averaged hydroxyl mixing ratio at 67.5° N for summer solstice, which is strongly modulated by the solar cycle.

The chemical heating is a very important diabatic heating source influencing the

thermal conditions under which NLC will be formed. One could expect that a decline of the odd oxygen concentrations should also reduce the chemical heating rate, but the concentrations of the odd hydrogen constituents increased at the same time, so this fact compensates the negative effect. The chemical heating is, in essence, determined by the stepwise recombination of atomic oxygen to molecular oxygen leaving its latent chemical energy at the place of recombination. The latent chemical energy is both downward transported from the thermosphere and locally created by the formation of O due to the dissociation of O_2. These processes are not directly affected by the increasing humidity. The photolysis of water vapor plays no great part in the energetic balance. The stepwise recombination of atomic oxygen takes place via the formation of ozone and both the formation of OH and HO_2 within the catalytic cycles. As a consequence, the height of recombination changes if the hydrogen radical concentration alters. This process depends on the vertical wind direction. As discussed above, the chemistry of the middle atmosphere represents an intricate nonlinear system. This system is characterized by different feedbacks. One of these mechanisms is connected with the production of chemical heat, which acts in two ways: it alters the wind system and particularly the vertical component, and changes the chemical reaction rates of the temperature-dependent reactions. Our calculations revealed two regions of strong influence. Figure 13 shows the absolute deviation of a diurnal chemical heating rate at 67.5° N between 1890 and 1997. The relative deviation of the chemical heating rate is less informative. The figure displays two regions marked by the strongest absolute changes occurring during summer. The first region is placed at the summer mesopause (between 87 and 91 km) and is characterized by the strongest increase of chemical heating rate. The most significant reactions for the chemical heat in the region 85–90 km are OH+O, O+HO_2 and O_3+H. Hence, the increase of the chemical heating rate in this region is caused by the rising humidity in the mesopause region due to the enhanced odd-hydrogen production; however, this is damped by the fact that the odd oxygen concentrations decrease with increasing odd hydrogen concentrations. A changed thermal regime feeds back to the wind system and influences the chemi-

cal reaction rates. The second region of strongest absolute deviation is located close to the stratopause and has a negative sign. The main reaction of the production of chemical heat in the stratopause region is given by the three-body reaction $O+O_2+M$. Its reaction rate increases with decreasing temperature. Consequently, the system is characterized by negative feedback in both regions. Figure 14 shows the latitudinal behavior of the absolute deviation of the diurnal chemical heating rate near north summer solstice (1 July). The figure illustrates the latitudinal extension of both regions. The trend of chemical heating rate has negative sign from equator to approximately 50° N for all heights during summer season, but it change the sign from 50° N to north pole in mesopause region. This feature will be discussed below.

6.2 Impacts due to the CO_2 increase

The most spectacular anthropogenic increase of a minor constituent is that of CO_2. As mentioned, we only briefly consider the change of the mesospheric chemistry owing to the CO_2 increase and neglect the influence of the thermal regime of the middle atmosphere. There are some contributions dealing with the impact of a CO_2 doubling on the thermal regime of the upper atmosphere (e.g., Berger and Dameris, 1993; Keating et al., 2000; Bremer and Berger, 2002), but no study additionally considers the response of the chemistry in the MLT region. Figure 15 shows the relative deviation of the CO concentration for 1 April. The increase of the CO mixing ratio depends on height, but also on latitude and season. The lifetime of CO is relatively long (for $[OH]=10^7\ cm^{-3}$ results 6.67×10^5 s). The impact on the composition of the hydrogen radicals is very small and not shown here as only a radical conversion takes place from OH to H and no radical loss occurs. However, the distribution of OH influences the mixing ratio of CO. The figure displays a generally negative trend in the stratosphere. The reason is the fact that the production of OH increased essentially more between 1890 and 1997 than did CO in the stratosphere, so the loss by OH is more efficient than the increased formation of CO by the photolysis of CO_2. In the mesosphere the picture is not uniform. Although CO increased in most regions, there are distinct domains of a small inverse

trend resulting from larger OH-concentrations.

7 Discussion

One of the most interesting questions is, how much the change of the composition of atmospheric minor constituents influenced the condition for the formation of ice particles in the NLC region, meaning the conditions in the summery high latitudes. The temperature has the most important influence on the creation of NLCs and PMSEs. It is assumed to be dropped in the middle atmosphere due to the amplified radiative cooling by increased CO_2 concentration. However, the cooling is not a homogeneous process affecting all altitudes in the same way. A mysterious fact is the finding that the height of the NLC has not noticeably declined since the time of first observation in 1883 (Jesse, 1885, 1891; von Zahn and Berger, 2003). The term "equithermal submesopause" was introduced by Lübken et al. (1996) and reflect significant repeatability mean mesopause temperature during last 40 years and the NLC height since first observation. Recently, Lübken (2001) found no temperature trend in the mesosphere in high latitudes in summer. These are unexpected findings not simple to interpret. A cooling of the whole middle atmosphere should shift the levels of constant air density downward, as assumed in the papers about the change of the radio-wave reflection height using the technique of the phase-height measurement (e.g., Taubenheim, 1997; Bremer, 1997, 2001; Bremer and Berger, 2002). In the mesopause region, the concrete height is decisive for the sign of the temperature change if the levels of constant air density decline. For a height above the mesopause (defined by the temperature minimum), the temperature increases owing to its positive gradient and may be compensated by a cooling trend in the vicinity of the considered height. Below the mesopause, according to the negative temperature gradient, the temperature decreases. The degree of supersaturation is given by the Clausius-Clapeyron Equation. A drop of the levels of constant pressure also entails a decrease of the partial pressure of water vapor. At a constant height, this could be compensated by the increasing humidity. Both influences, the de-

crease of temperature and rise of humidity, should increase the occurrence rate of NLC, as indeed has been observed since the time of their first observation (e.g., Gadsden, 1998). The only question is why this did not lower their lower border, which is located below the mesopause. The explanation, possibly, is that the positive trend of chemical heating rate at high latitude in mesopause (Figs. 13 and 14) partially compensate the cooling due to CO_2 increase. These both processes are in competition and the result is the absence of temperature trends in mesopause at high latitudes during the summer, as it was found by Lübken (2001). Thus, the chemical heat can play a role in stabilizing of mesopause and formation of "equithermal submesopause" at high latitudes in summer. In light of our calculations, at least in mesopause, there is no a contradiction between measurements of Lübken (2001) and Hauchecorne et al. (1991), or Bremer and Berger (2002), which found in mesosphere and mesopause at mid latitudes (44° N and 50.7° N respectively) negative trends of temperature, because the trend of chemical heating rate at mid latitudes is negative for all altitudes during the summer (Fig. 14) and can not compensate the anthropogenic cooling. Apparently, this static picture is not comprising enough. The global polar anti-cyclone changes and with it the complete circulation. Possible weakening of the upward vertical wind as a result of the cooling of the underlying atmosphere decreases the adiabatic cooling. The collision between CO_2 and O seems to be an efficient cooling process (Crutzen, 1970). A reduction of the atomic oxygen concentration also makes this cooling process more inefficient. We mentioned already that the change of the chemical heating rate tends to increase in that area and season. Breaking gravity waves are a rather important diabatic heating source controlled by processes in the lower atmosphere which are subjected to climatic change. Normally, the models are tuned by a more or less arbitrary spectrum of gravity waves so that a required global temperature distribution results. Also, the propagation of planetary waves and, in the winter season, the occurrence of sudden stratospheric warming influences the thermal regime of the mesopause region. This enumeration of influences and the brief discussion of them make clear that no simple answer can be given. In order to investigate the trend of the conditions in the NLC region, at least, an

interactive operating model is required considering all essential processes. We also expect an increase of the occurrence rate of NLC with increasing humidity, as suggested by Thomas et al. (1989).

The most important change of the chemically active minor constituents may concern OH in the OH-layer. The airglow in the Meinel bands system is used by different groups to derive the temperature and for analysis of gravity waves (Taylor and Garcia, 1995; Taylor, 1997; Taylor et al., 1998), but OH itself is also a subject of investigation (e.g., Offermann and Gerndt, 1990; Summers et al., 1996; Bittner et al., 2002). The Meinel bands airglow layer results mainly from the reaction $O_3+H \rightarrow OH^*+O_2$. The main loss process of the vibrationally excited states is quenching by air particles. The chief loss of OH is the reaction with atomic oxygen. Since O decreases with decreasing height but the air density increases, the OH-layer lies somewhat lower than the OH*-layer. Considering the production term of OH*, H increases but O_3 decreases, reducing the airglow layer. Depending on season, latitude and vibrational number, the calculations show 20–50% decrease of the OH* concentration with saving the same altitude of the layer over the years. Thus, airglow measurements can be applied for the study of anthropogenic changes in mesopause. In contrast to this finding, the OH-layer became more pronounced owing to the decline of the loss term by reaction with O. Simultaneously, the height of the OH-layer increased.

The ozone decrease in the mesopause region was an expected effect due to the amplified first catalytic cycle including H and OH as catalysts. Below the mesopause, the system tends to respond in a nonlinear manner. However, it is impossible to give a definitive answer on the basis of a relatively coarse integration procedure, so an improved investigation is necessary. The chemical reasons for a possible trigger solution just around the ozone minimum at 80 km were discussed in Hartogh et al. (2004). Yang and Brasseur (1994) showed its existence in a very simplified model. Certainly, the ozone decrease in the stratopause region is more important. Different groups discussed the so-called ozone deficit problem (e.g., Eluszkiewicz and Allen, 1993; Siskind et al., 1995) consisting of a systematic underestimation of ozone by the standard mod-

els only in the stratopause region (upper stratosphere-lower mesosphere). Crutzen et al. (1995) did not find a deficit. This finding points to the fact that the ozone determining processes are not completely understood. We mentioned already that the second catalytic cycle is responsible for the decrease if the humidity increases. This cycle acts, of course, in the whole atmosphere, but hydrogen radicals increase faster toward the stratopause than atomic oxygen decreases. A second fact has to be taken into consideration: namely, the positive feedback between ozone and the ozone dissociation rate. This effect was first taken into calculation in Sonnemann et al. (2005b). The ozone dissociation rate is determined by the absorption of the radiation of ozone itself. This is the so-called self-shielding effect. An ozone decrease enhances the radiation dissociating ozone, which amplifies further ozone destruction in the domain where the ozone dissociation rate declines the most with decreasing height. This is approximately the altitude below 60 km, including the extended stratopause region. Above this height a change of ozone has no large absorption effect. This feedback is usually not considered in the models, but the measurements reflecting the reality contain this effect. A decrease of ozone by 10 to 14% just at the stratopause but not above this domain up to 75 km was inferred from microwave measurements in Lindau (52.66° N, 10.13° E), if comparing the observations with the ozone reference model derived from SME-satellite measurements 20 years earlier. This finding could be an indication of an increasing humidity in the latest 20 years. In the upper domain around the mesopause, the solar influence is essentially stronger and the relations are exceedingly more complicated than at the stratopause.

8 Summary

We investigated the influence of the rising concentrations primarily of methane, but also of dinitrogen oxide and carbon dioxide since the pre-industrial era. We used for calculations our global 3D-model COMMA-IAP designed for the exploration of the MLT-region and particularly the extended mesopause region. We derived a quadratic fit

using the sunspot number available since 1749 as the only solar proxy for the Lyman-α flux before 1947, and calculated the solar Lyman-α flux back to the pre-industrial time. The fit was based on Lyman-α flux values derived by Woods et al. (2000) available since 1947. The calculated Lyman-α flux values have been utilized to determine the water vapor dissociation rate. The water vapor trend analysis is based on estimated methane trends since the pre-industrial era. We took into calculation an exponential increase of methane. An unsolved and intricate problem for the model calculations consists of the water vapor mixing ratio at the hygropause during the time range of trend calculation. We assumed that the hygropause was dryer at the pre-industrial time than presently and used a very conservative value of 10%. The methane oxidation results in a more humid middle atmosphere. According to the rising methane concentration that yields two water vapor molecules per methane molecule, but the increase depends on height, season and solar activity. A small time delay of a few years is caused by the slow transport through the middle atmosphere. The solar influence on the water vapor mixing ratio due to the variation of the Lyman-α radiation is insignificant below about 80 km within summery high latitudes, but it becomes increasingly more important above this altitude. The increasing water vapor concentration should impact the NLC occurrence rate, but the relations in the mesopause region are very intricate. The rising water vapor concentrations enhance the hydrogen radical concentrations and these reduce the mesospheric ozone, particularly in the mesopause region, owing to catalytic odd oxygen destruction processes. A second region of stronger ozone decrease is located in the vicinity of the stratopause. This model assertion was confirmed by microwave measurements of ozone in middle latitude at Lindau, Germany when comparing the observations with data of the ozone reference model established from satellite measurements 20 years ago. Another influence of increasing hydrogen radical concentrations concerns the OH-layer, which became more pronounced and the maximum height increased a little. The change of the chemical heating rate was discussed. In the mesopause region the chemical heating rate increased whereas it decreased in the stratopause region. The positive trend of chemical heating rate at

high latitude in mesopause during the summer can play a role of stabilizing mechanism and can be one of the reasons of "equithermal submesopause". In this paper we did not consider the change of NO_x due to the increasing N_2O concentrations.

Increasing CO_2 concentrations somewhat increase the CO content of the mesosphere with the exception of some regions where CO slightly decreases. In these areas the increase of OH over-compensates for the rise of CO. The influence of CO upon the chemistry is very small. This is also valid for the impact of the NO_x chemistry upon the odd oxygen-odd hydrogen system of the MLT region. The main effect of increasing carbon dioxide is connected with a cooling of the upper atmosphere. The trend analysis revealed a decrease of CO in the stratosphere as a result of relatively stronger growth of OH as the only CO destroyer. The cooling, and consequently the change of the dynamics and the chemical reaction rates, is not considered in the model. A model run of 120 years is very computer time consuming. That is why we had to choose a relatively large time step (15 min). A bistable state of the chemistry around 80 km hints of a nonlinear response, but this effect has to be investigated in more detail. The model does not run interactively, so the annual variations of the dynamical fields did not change from year to year over the calculated period. Hence, all trends result from the chemistry and, to a small extent, from the variation of the Lyman-α radiation.

Acknowledgements. This work was supported by the Deutsche Forschungsgemeinschaft (DFG) grant So268/4.

References

Angione, R. J., Mederios, E. J., and Roosen, R. G.: Stratospheric ozone as viewed from the Chappuis band, Nature, 261, 289–290, 1976.

Berger, U.: Numerische Simulation klimatologischer Prozesse und thermische Gezeiten in der mittleren Atmosphäre, Thesis, Univ. Cologne, Germany, 1994.

Berger, U. and Dameris, M.: Cooling of the upper atmosphere due to CO_2 increases: a model study, Ann. Geophys., 11, 809–819, 1993, http://www.ann-geophys.net/11/809/1993/.

Berger, U. and von Zahn, U.: The two-level structureof the mesopause: A model study, J. Geophys. Res., 104, 22 083–22 093, 1999.
Bittner, M., Offermann, D., Graef, H.-H., Donner, M., and Hamilton, K.: An 18 year time series of OH rotational temperatures and middle atmosphere decadal variations, J. Atmos. Sol. Terr. Phys., 64, 1147–1166, 2002.
Bremer, J.: Long-term trends in the meso- and thermosphere, Adv. Space Res., 20, 2075–2083, 1997.
Bremer, J.: Trends in the thermosphere derived from global ionosonde observations, Adv. Space Res., 28, 997–1006, 2001.
Bremer, J. and Berger, U.: Mesospheric temperature trends derived from ground-based LF phase-height observations at mid-latitudes: comparison with model simulations, J. Atmos. Sol. Terr. Phys., 64, 805–816, 2002.
Crutzen, P. J.: Discussion of paper "Absorption and emission by cabon dioxide in the atmosphere", edited by: Houghton, J. T., Q. J. R. Meteorol. Soc., 96, 767, 1970.
Crutzen, P. J., Grooss, J.-U., Bruehl, C., Mueller, R., and Russel III, J. M.: A reevaluation of the ozone budget with HALOE UARS data: No evidence of the ozone deficit, Science, 268, 705–708, 1995.
Dlugokencky, E. J., Houweling, S., Bruhwiler, L., Masarie, K. A., Lang, P. M., Miller, J. B., and Tans, P. P.: Atmospheric methane levels off: Temporary pause or a new steady-state?, Geophys. Res. Lett., 30, 1992, doi:10,1029/2003GL018126, 2003.
Ebel, A., Berger, U., and Krueger, B. C.: Numerical simulations with COMMA, a global model of the middle atmosphere, SIMPO Newsl., 12, 22–32, 1995.
Eluszkiewicz, J. and Allen, M.: A global analysis of the ozone deficit in the upper stratosphere and lower mesosphere, J. Geophys. Res., 98, 1069–1082, 1993.
Evans, S. J., Toumi, R., Harries, J. E., Chipperfield, M. P., and Russel, J. M.: Trends in stratospheric humidity and the sensitivity of ozone to these trends, J. Geophys. Res., 103, 8715–8725, 1998.
Fogle, B.: Noctilucent clouds over North America, Nature, 207, 696–698, 1965.
Foster, P. M., de F. and Shine, K. P.: Stratospheric water vapour changes as a possible contributor to observed stratospheric cooling, Geophys. Res. Lett., 26, 3309–3312, 1999.
Gadsden, M.: The North-West Europe data on noctilucent clouds: A survey, J. Atmos. Terr. Phys., 60, 1163–1174, 1998.
Hartogh, P.: High resolution chirp transform spectrometer for middle atmospheric microwave

sounding, in: Satellite Remote Sensing of Clouds and the Atmosphere II, edited by: Haigh, J. D., Vol. 3220 of Proc. SPIE, 115–124, 1997.
Hartogh, P. and Hartmann, G. K.: A high resolution chirp transform spectrometer for microwave measurements, Meas. Sci. Technology, 1, 592–595, 1990.
Hartogh, P. and Jarchow, Ch.: Ground-based detection of middle atmospheric water vapour, Global Process Monitoring and Remote Sensing of the Ocean and Sea Ice, edited by: Deering, D. W. and Gudmandsen, P., Vol. 2586 of Proc. SPIE, pp 188–195, 1995.
Hartogh, P., Hartmann, G. K., and Zimmermann, P.: Simultaneous water vapor and ozone measurements with millimeter-waves in the stratosphere and mesosphere, IEEE Catalog Number 91CH2971-0, 1, 227–230, 1991.
Hartogh, P., Jarchow, Ch., Sonnemann, G. R., and Grygalashvyly, M.: On the spatiotemporal behavior of ozone within the upper mesosphere/mesopause region under nearly polar night conditions, J. Geophys. Res., 109, D18303, doi:10.1029/2004JD004576, 2004.
Hauchecorne, A., Chanin, M.-L., and Keckhut, P.: Climatology and trends of the middle atmospheric temperature (33–87 km) as seen by Rayleigh Lidar over the south of France, J. Geophys. Res., 96, 15 297–15 309, 1991.
Jesse, O.: Auffallende Abenderscheinung am Himmel, Meteorol. Z., 2, 311–312, 1885.
Jesse, O.: Untersuchungen über die sogenannten leuchtenden Nachtwolken, Meteorol. Z., 8, 306–308, 1891.
Keating, G. M., Tolson, R. H., and Bradford, M. S.: Evidence of long-term global decline in the Earth's thermospheric density apparently related to anthropogenic effects, Geophys. Res. Lett., 27, 1523–1526, 2000.
Khalil, M. A. K., Rasmussen, R. A., and Moraes, F.: Atmospheric methane at Cap Meares: Analysis of a high-resolution data base and its environmental implications, J. Geophys. Res., 98, 14 753–14 770, 1993.
Körner, U. and Sonnemann, G. R.: Global 3D-modeling of water vapor concentration of the mesosphere/mesopause region and implications with respect to the NLC region, J. Geophys. Res., 106, 9639–9651, 2001.
Kremp, Ch., Berger, U., Hoffmann, P., Keuer, D., and Sonnemann, G. R.: Seasonal variation of middle latitude wind fields of the mesopause region – a comparison between observation and model calculation, Geophys. Res. Lett., 26, 1279–1282, 1999.
Lübken, F.-J., Fricke, K.-H., and Langer, M.: Noctilucent clouds and the thermal structure near the Arctic mesopause, J. Geophys. Res., 101, 9489–9508, 1996.

Lübken, F.-J.: No long term change of the thermal structure in the mesosphere at high latitudes during summer, Adv. Space Res., 28(7), 947–953, 2001.
Offermann, D. and Gerndt, R.: Upper mesospheric temperatures from OH* emissions, in CIRA 1986, Part II, eds. Rees, D., Barnett, J. J., and Labitzke, K., Adv. Space Res., 10(12), 217–221, 1990.
Oldmans, S. J. and Hofmann, D. J.: Increase in lower stratospheric water vapour and a midlatitude northern hemisphere site from 1981-1994, Nature, 374, 146–149, 1995.
Schröder, W.: Were noctilucent clouds caused by the Krakatoa eruption?, Bull. Am. Meteor. Soc., 112, 2081–2085, 1999.
Seele, C. P. and Hartogh, P.: Water vapor of the polar middle atmosphere: Annual variation and summer mesospheric conditions as observed by ground-based microwave spectroscopy, Geophys. Res. Lett., 26, 1517–1529, 1999.
Simon, P. C.: Solar irradiance between 120 and 400 nm and its variation, Solar Physics, 74, 273–291, 1981.
Siskind, D. E., Connor, B. J., Eckman, R. S., Remsberg, E. E., Tsou, J. J., and Parrish, A.: An intercomparison of model ozone deficits in the upper stratosphere and mesosphere from two data sets, J. Geophys. Res., 100, 11 191–11 201, 1995.
Sonnemann, G. R. and Körner, U.: The total hydrogen mixing ratio anomaly around the mesopause region, J. Geophys. Res., 108, 4692, doi:10.1029/2002JD003015, 2003.
Sonnemann, G., Kremp, Ch., Ebel, A., and Berger, U.: A three-dimensional dynamic model of minor constituents of the mesosphere, Atmos. Environ., 32, 3157–3172, 1998.
Sonnemann, G. R. and Grygalashvyly, M.: Solar influence on mesospheric water vapor with impact on NLCs, J. Atmos. Sol. Terr. Phys., 67, 177–190, 2004.
Sonnemann, G. R. and Grygalashvyly, M.: On the two-day oscillation and the day-to-day variability in global 3-D-modeling of the chemical system of the upper mesosphere/mesopause region, Nonlin. Proc. Geophys., 12, 691–705, 2005.
Sonnemann, G. R., Grygalashvyly, M., and Berger, U.: Autocatalytic water vapor production as a source of large mixing ratios within the middle to upper mesosphere, J. Geophys. Res., 110, D15303, doi:10.1029/2004JD005593, 2005a.
Sonnemann, G. R., Hartogh, P., and Grygalashvyly, M.: Nonlinear response of the ozone chemistry within the stratopause and mesopause region under realistic conditions, Proc. Int. Symp.: Topical Problems of Nonlinear Wave Physics NWP-2005, Nonlinear Phenomena in Environmental Research (NWP-3), pp. 108–109, St. Petersburg – Nizhny Novgorod, Russia,

2–9 August 2005b.
Summers, M. E., Conway, R. R., Siskind, D. E., Bevilacqua, R., Strobel, D. F., and Zasadil, S.: Mesospheric HO_x photochemistry: Constraints from recent satellite measurements of OH and H_2O, Geophys. Res. Lett., 23, 2097–2100, 1996.
Taubenheim, J., Entzian, G., and Berendorf, K.: Long-term decrease of mesospheric temperature, 1963–1995, inferred from radiowave reflection heights, Adv. Space Res., 20(11), 2059–2063, 1997.
Taylor, M. J.: A review of advances in imaging techniques formeasuring short period gravity waves in the mesosphere and lower thermosphere, Adv. Space Res., 19, 667–676, 1997.
Taylor, M. J. and Garcia, F. J.: A two-dimensional spectral analysis of short period gravity waves imaged in the OI(557.7 nm) and near infra red OH nightglow emissions over Arecibo, Puerto Rico, Geophys. Res. Lett., 22, 2473–2476, 1995.
Taylor, M. J., Seo, S. H., Nakamura, T., Tsuda, T., Fukunishi, H., and Takahashi, Y.: Long baseline measurements of short-period mesospheric gravity waves during the SEEK campaign, Geophys. Res. Lett., 25, 1797–1800, 1998.
Thomas, G. E., Olivero, J. J., Jensen, E. J., Schröder, W., and Toon, O. B.: Relation between increasing methane and the presence of ice clouds at the mesopause, Nature, 338, 490–492, 1989.
Thomas, G. E. and Olivero, J. J.: Noctilucent clouds as possible indicators of global change in the mesosphere, Adv. Space Res., 28(7), 937–946, 2001.
Vidal-Madjar, A.: Evolution of the solar Lyman alpha flux during four consecutive years, Solar Physics, 40, 69-86, 1975.
Vidal-Madjar, A.: The solar spectrum at Lyman-alpha 1216 Å, in: *The Solar Output and its Variation*, edited by O. R. White, Colo. Assoc. Univ. Press, Boulder, 213–236, 1977.
Vidal-Madjar, A. and Phissamay A.: The solar Lα flux near solar minimum, Solar Physics, 66, 227–271, 1980.
von Zahn, U., Höffner, J., Eska, V., and Alpers, M.: The mesopause altitude: Only two distinctive levels worldwide?, Geophys. Res. Lett., 23, 3231–3234, 1996.
von Zahn, U. and Berger, U.: The altitude of noctilucent clouds: Groundbased observations and their interpretation through numerical modeling, in Proceedings of the 16th ESA Symposium on European Rocket and Balloon Programmes and Related Research, St. Gallen, Switzerland, ESA SP-530, edited by Warmbein, B., 295–301, 2003.
Woods, T. N., Tobiska, W. K., Rottman, G. J., and Worden, J. R.: Improved solar Lyman α

irradiance modeling from 1947 through 1999 based on UARS observations, J. Geophys. Res., 105, 27 195–27 215, 2000.
World Meteorological Organization (WMO), Scientific Asseessment of Ozone Depletion:1998, Geneva, 1999.
Yang, P. and Brasseur, G.: Dynamics of the oxygen-hydrogen system in the mesosphere, 1. Photochemical equilibria and catastrophe, J. Geophys. Res., 99, 20 955–20 965, 1994.

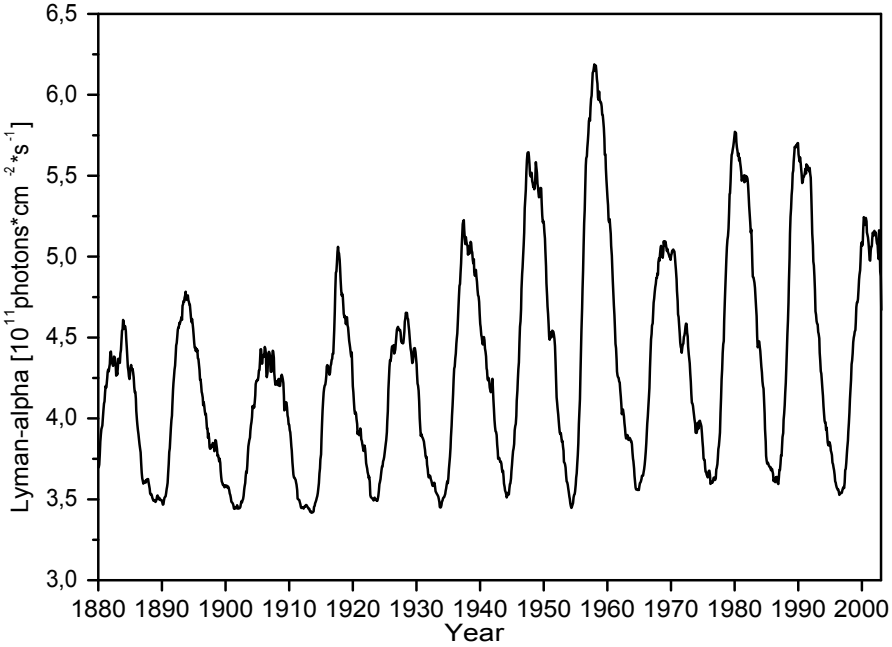

Fig. 1. Lyman-α flux reconstruction back to the time of first observations of NLC.

ACPD
7, 15453–15494, 2007

EGU

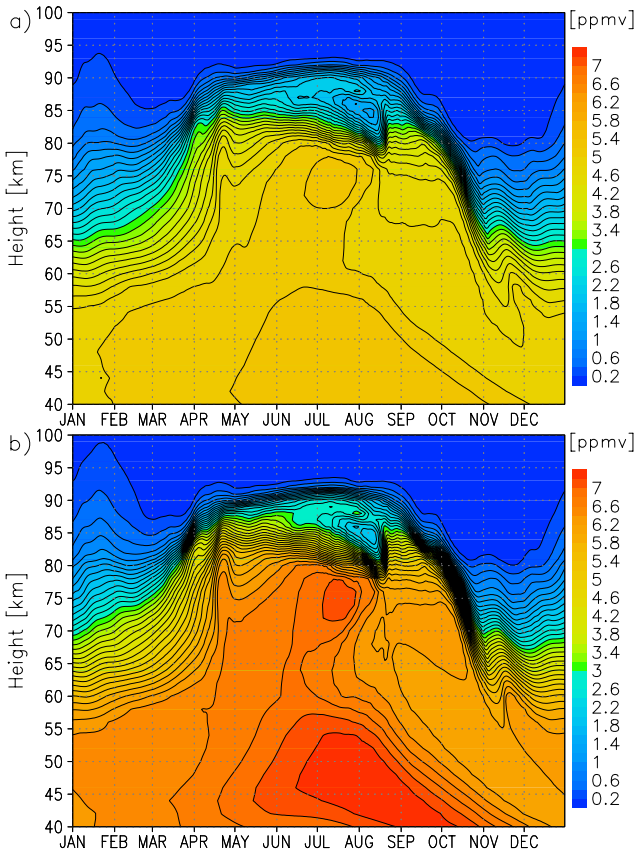

Fig. 2. Annual variation of the diurnally averaged water vapor mixing ratio at 67.5° N in 1890 **(a)** and in 1997 **(b)** calculated by means of COMMA-IAP.

ACPD
7, 15453–15494, 2007

EGU

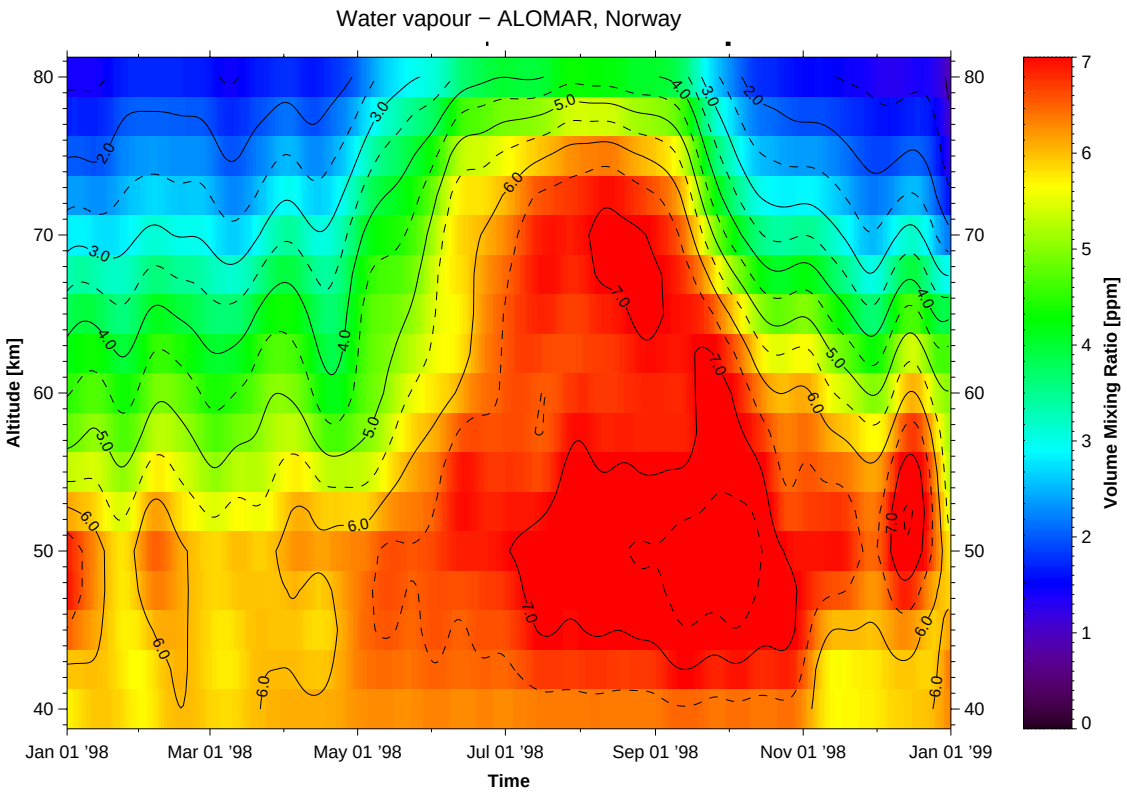

Fig. 3. Microwave measurements of water vapor in ALOMAR, Norway (69.29° N), in 1998.

ACPD
7, 15453–15494, 2007

EGU

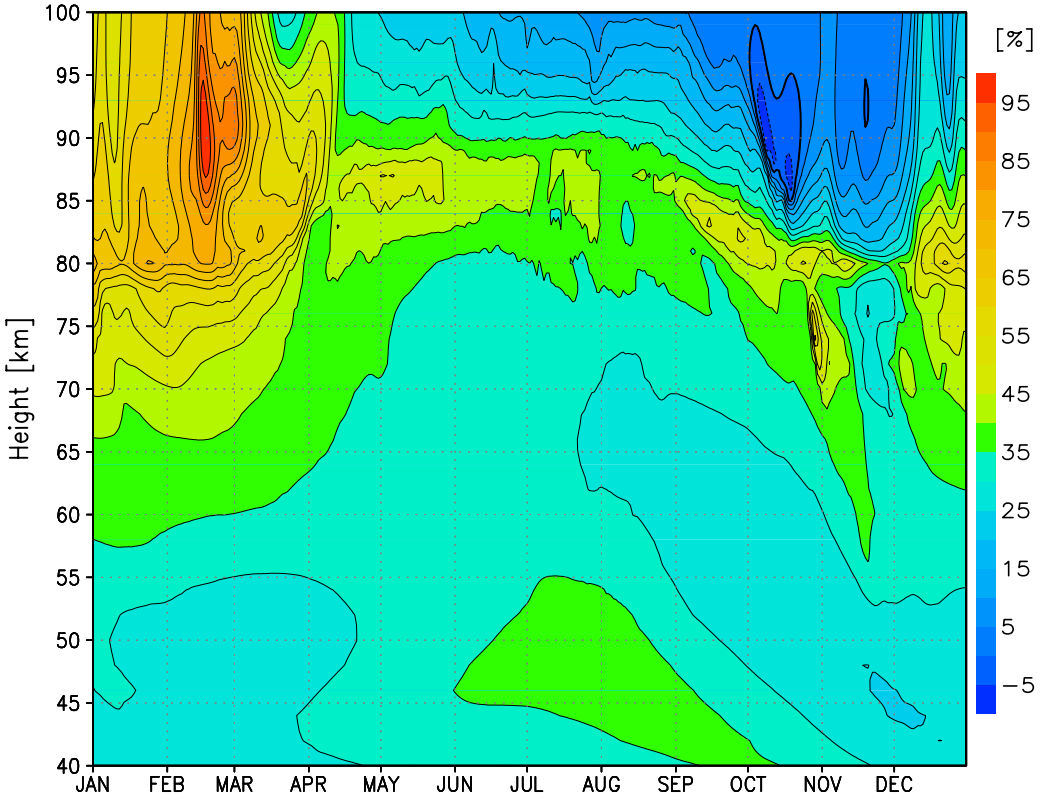

Fig. 4. Annual variation of the relative deviation of diurnally averaged water vapor between 1997 and 1880 at latitude of 67.5° N.

ACPD
7, 15453–15494, 2007

EGU

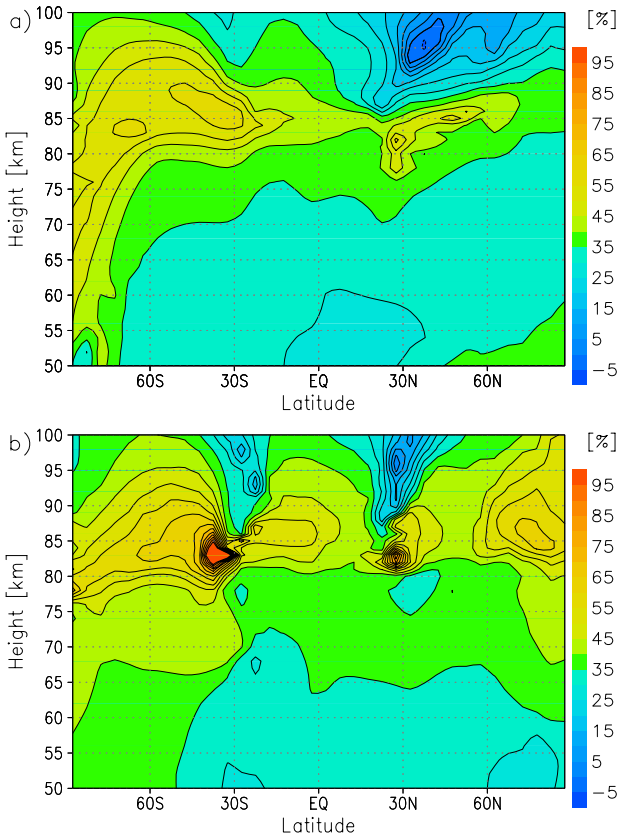

Fig. 5. Relative deviation of diurnally averaged water vapor mixing ratio between 1997 and 1890 in an altitude-latitude section for north summer solstice **(a)** and for spring equinox **(b)**.

ACPD
7, 15453–15494, 2007

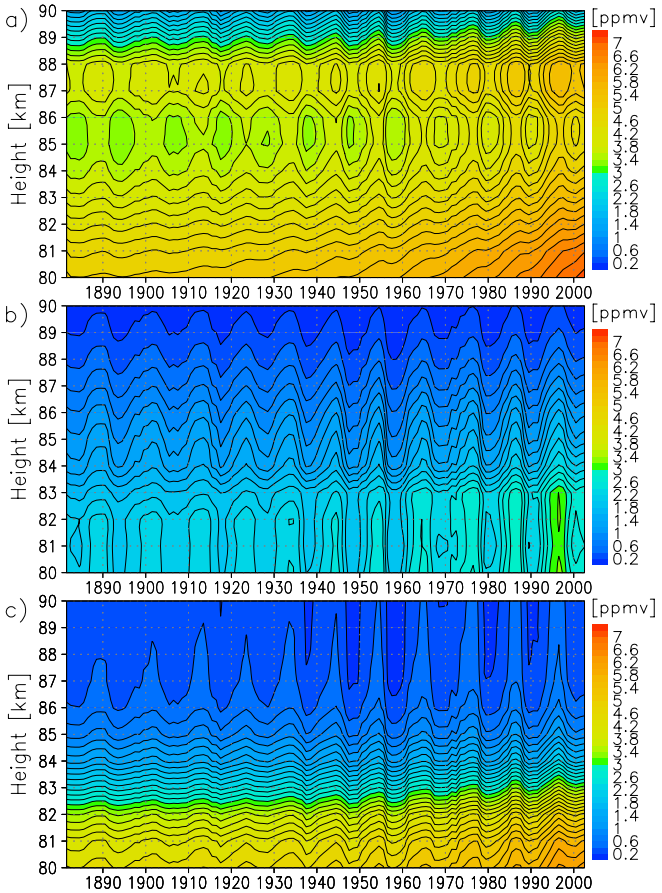

Fig. 6. Trend of the water vapor mixing ratio at midnight near summer solstice (1 July) for 67.5° N **(a)**, 42.5° N **(b)** and 2.5° N **(c)**.

ACPD
7, 15453–15494, 2007

EGU

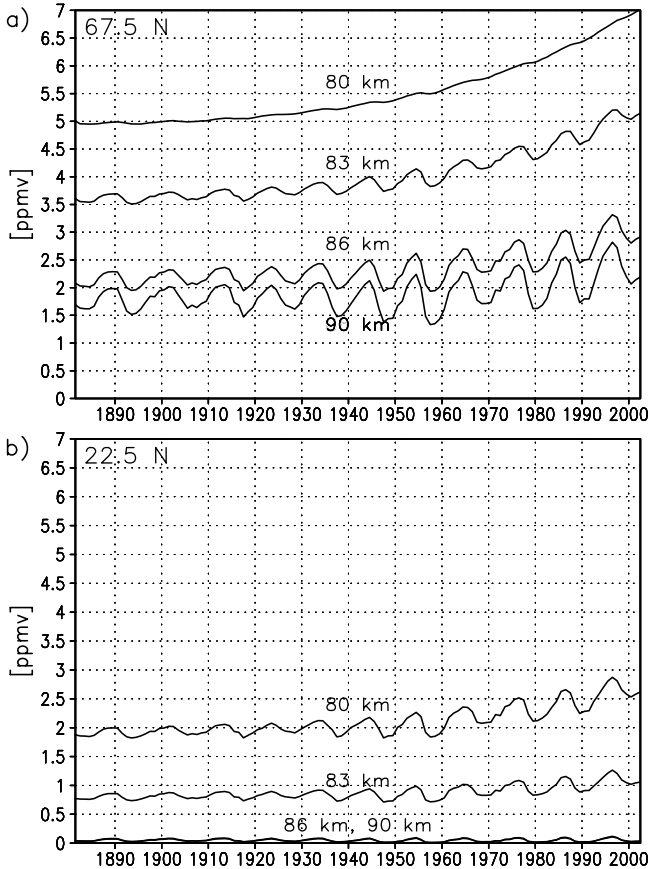

Fig. 7. Trend of diurnally averaged water vapor mixing ratio for summer solstice (1 July) at 67.5° N **(a)** and 22.5° N **(b)**.

ACPD
7, 15453–15494, 2007

EGU

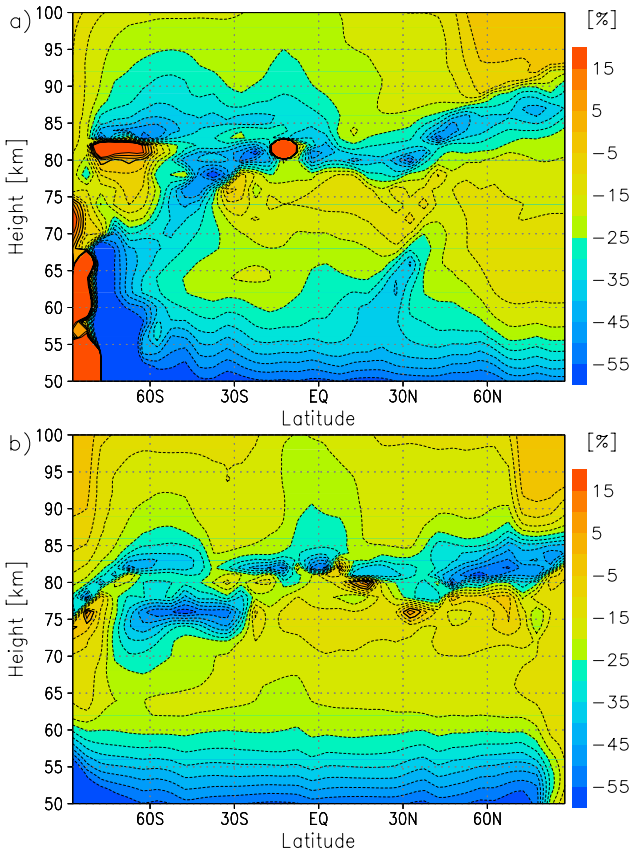

Fig. 8. Relative deviation of the diurnally averaged ozone mixing ratio in an altitude-latitude section for north summer solstice **(a)** and north spring equinox **(b)**.

ACPD
7, 15453–15494, 2007

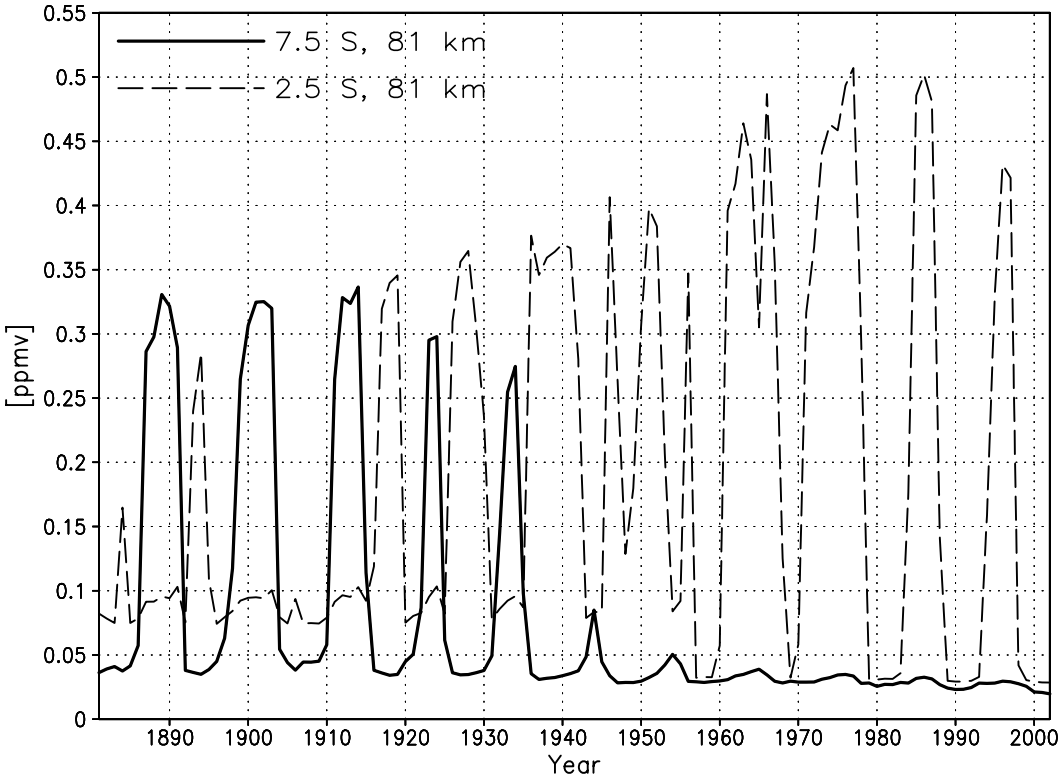

Fig. 9. Diurnally averaged ozone mixing ratio trends at 81 km at 2.5° S (dashed line) and 7.5° S (solid line) for the 1 January.

ACPD
7, 15453–15494, 2007

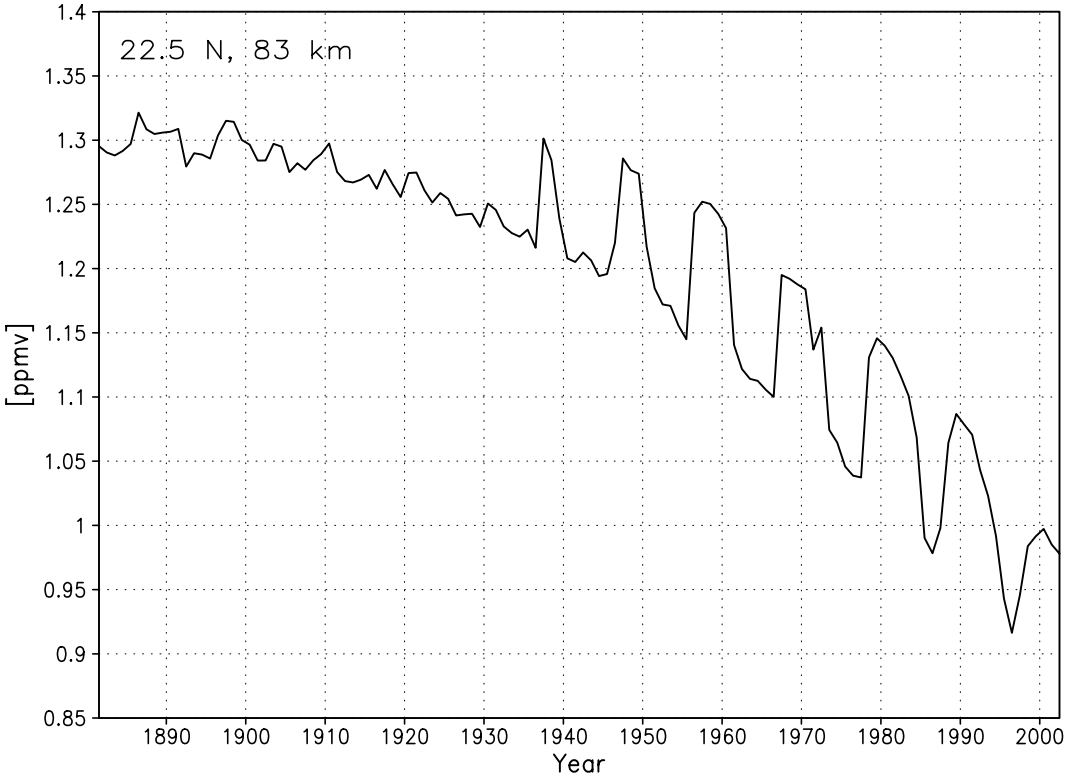

Fig. 10. Diurnally averaged ozone mixing ratio trend at 83 km height and 22.5° N for the 1 July.

ACPD
7, 15453–15494, 2007

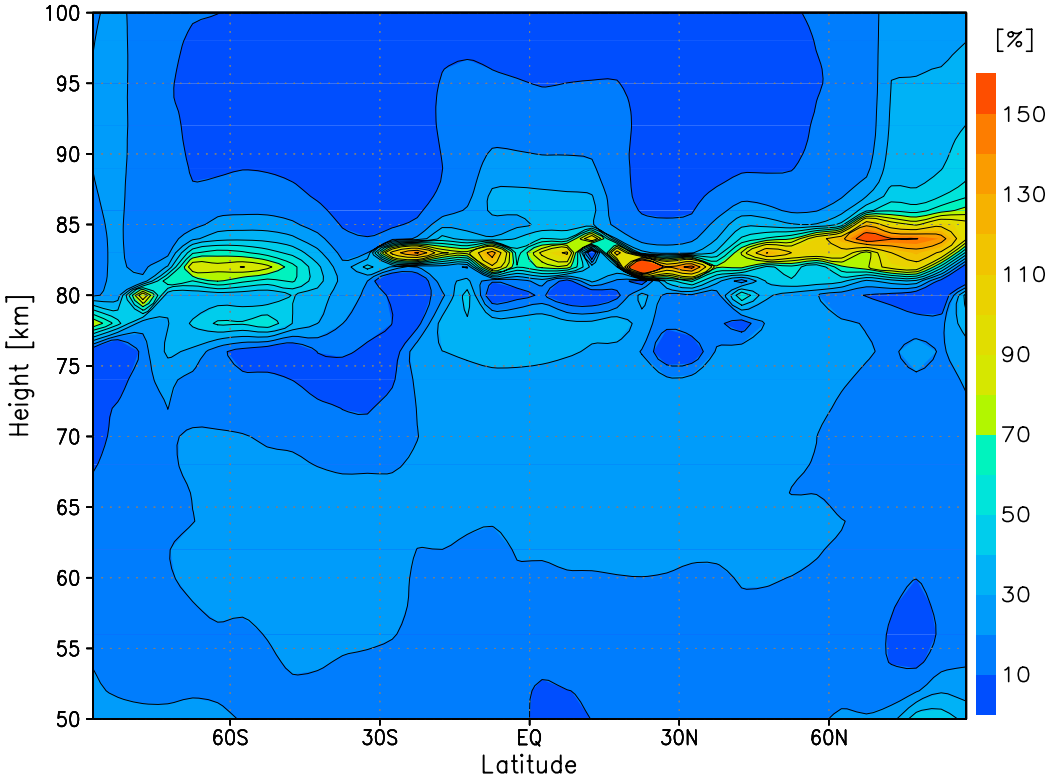

Fig. 11. Relative deviation of diurnally averaged hydroxyl mixing ratio in an altitude-latitude section for north spring equinox.

ACPD
7, 15453–15494, 2007

EGU

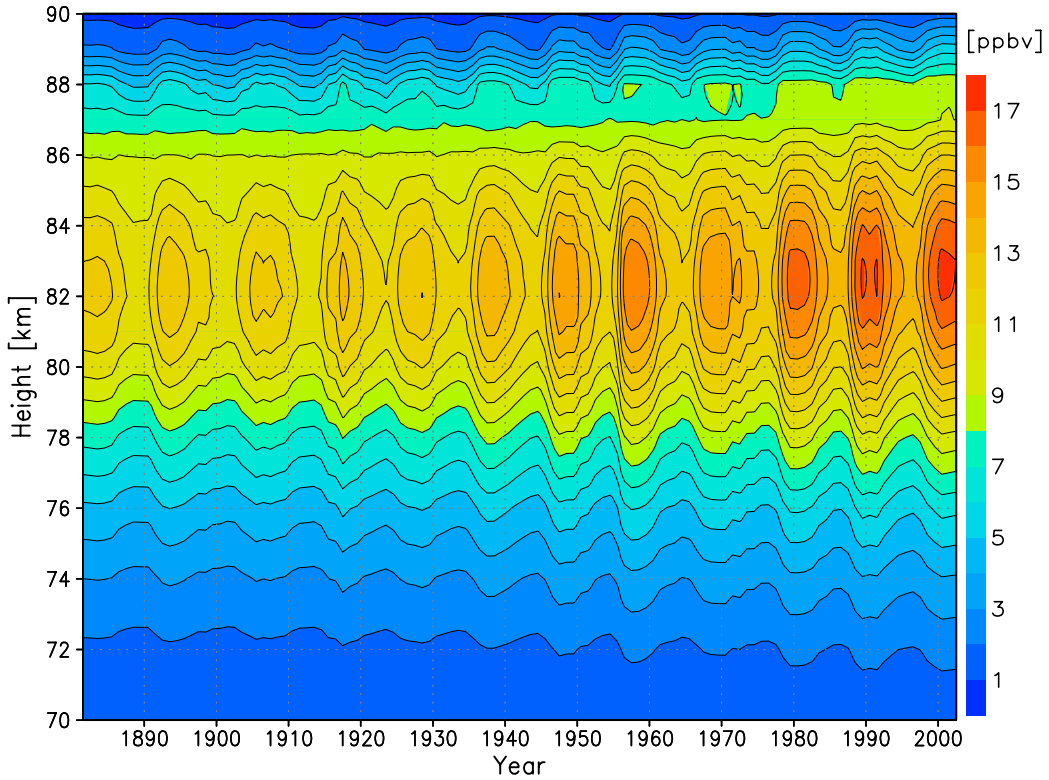

Fig. 12. Trend of the OH-layer at 67.5° N for north summer solstice (1 July).

ACPD
7, 15453–15494, 2007

EGU

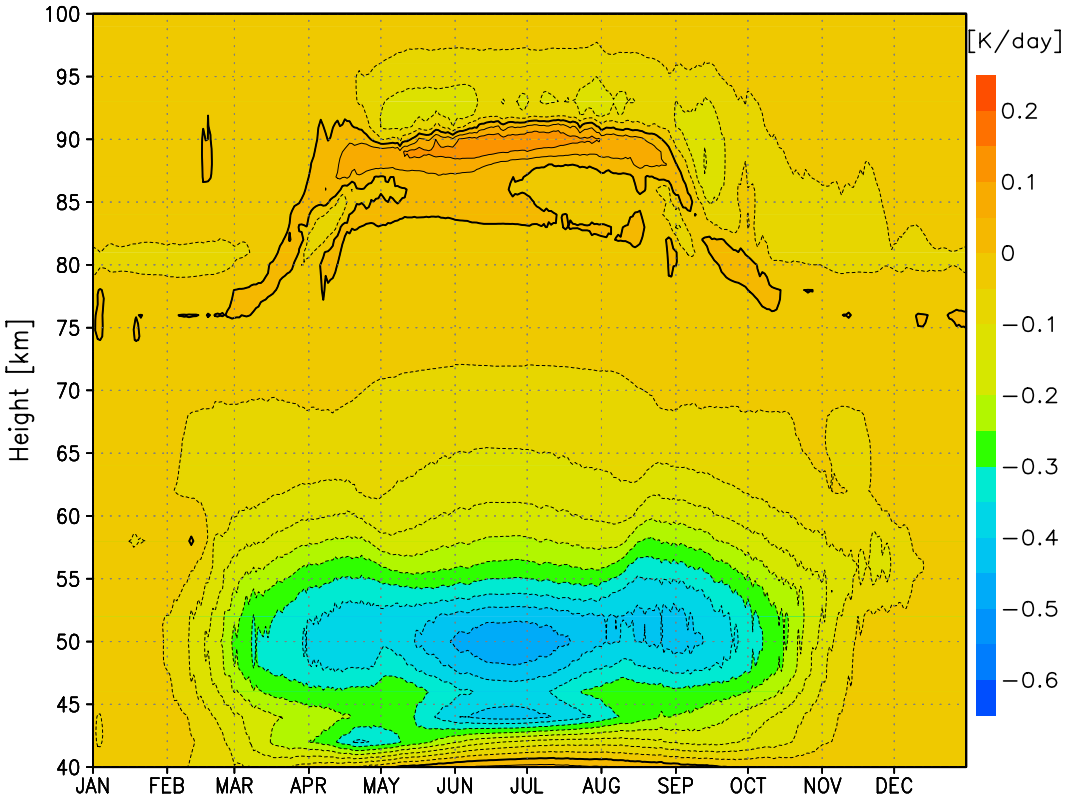

Fig. 13. Annual variation of absolute deviation of the chemical heating rate at 67.5° N.

ACPD
7, 15453–15494, 2007

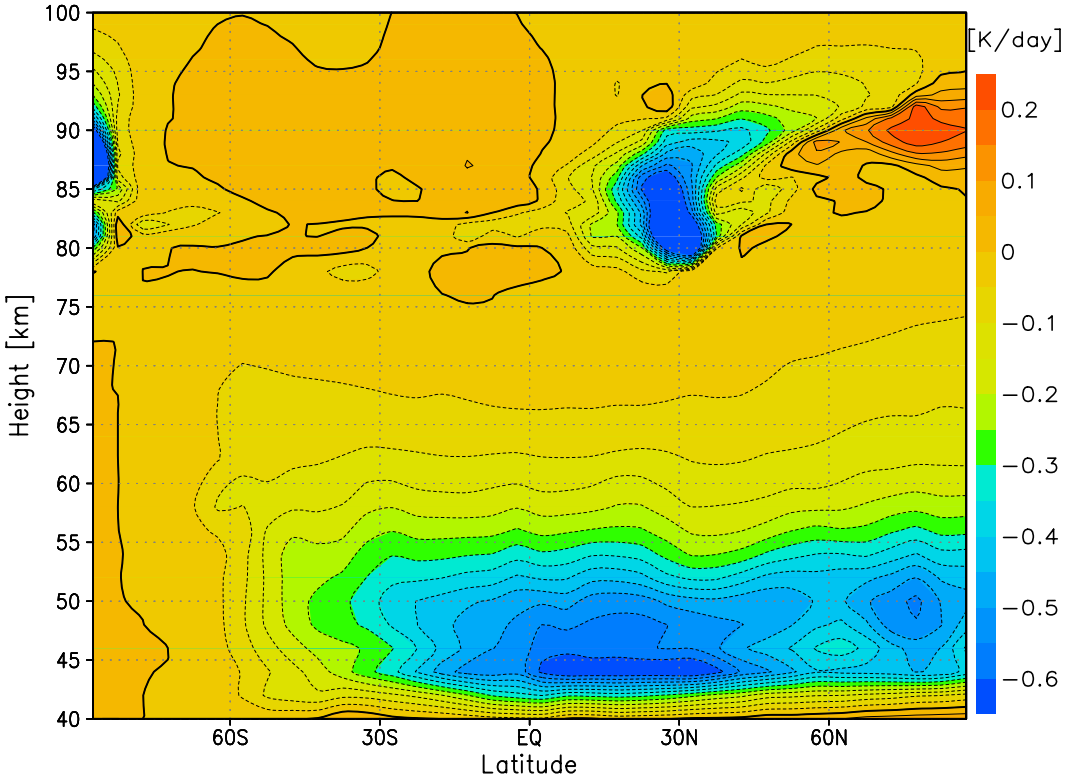

Fig. 14. Absolute deviation of the chemical heating rate for north summer solstice (1 July).

ACPD
7, 15453–15494, 2007

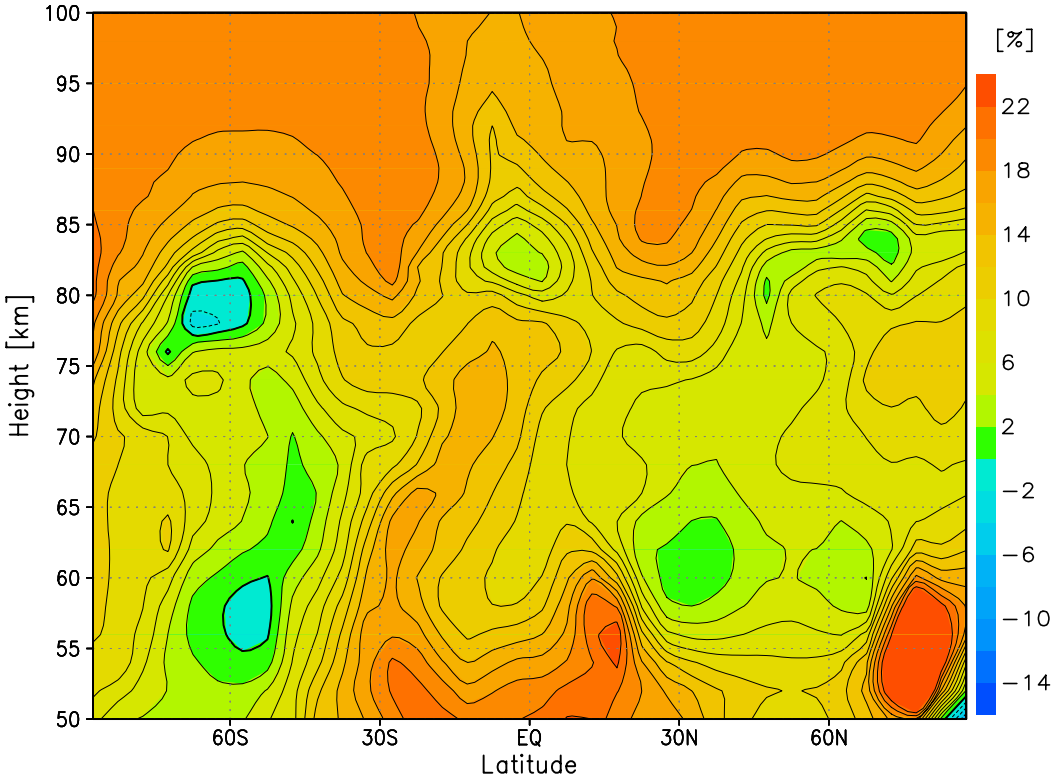

Fig. 15. Relative deviation of the diurnally averaged CO mixing ratio in a height-latitude section for the 1 April.

ACPD
7, 15453–15494, 2007

EGU